Journal of Zhejiang University-SCIENCE A (Applied Physics & Engineering)
ISSN 1673-565X (Print); ISSN 1862-1775 (Online)
www.zju.edu.cn/jzus; www.springerlink.com
E-mail: jzus@zju.edu.cn

Performance of a single-stage Linde-Hampson refrigerator operating with binary refrigerants at the temperature level of −60 °C*

Qin WANG, Kang CUI, Teng-fei SUN, Fu-sheng CHEN, Guang-ming CHEN[†‡]

(*State Key Laboratory of Clean Energy Utilization, Institute of Refrigeration and Cryogenics, Zhejiang University, Hangzhou 310027, China*)

[†]E-mail: gmchen@zju.edu.cn

Received Apr. 15, 2009; Revision accepted July 10, 2009; Crosschecked Dec. 9, 2009

Abstract: The optimization of the performance of a single-stage Linde-Hampson refrigerator (LHR) operating with six different binary refrigerants (R23/R134a, R23/R227ea, R23/R236ea, R170/R290, R170/R600a and R170/R600) with ozone depletion potentials (ODPs) of zero was conducted using a new approach at the temperature level of −60 °C. Among these binary refrigerants, the 0.55 and the 0.6 mole fractions of R23 for R23/R236ea are the most prospective nonflammable ones for the medium and low suction pressure compressors, respectively. For these two kinds of compressors, the 0.6 and the 0.65 mole fractions of R170 for R170/R600, respectively, are the most prospective binary refrigerants with low global warming potentials (GWPs). The results of optimization of pressure levels indicate that the optimum low pressure value for coefficients of performance (COP) is achieved when the minimum temperature differences occur at both the hot and the cold ends of the recuperator at a specified composition and pressure ratio. Two useful new parameters, the entropy production per unit heat recuperated and the ratio of heat recuperating capacity to the power consumption of the compression, were introduced to analyze the exergy loss ratio in the recuperator. The new approach employed in this paper also suggests a promising application even to the optimization of the performance with multi-component refrigerants.

Key words: Linde-Hampson, Binary refrigerant, Refrigerator, Performance, Optimization
doi:10.1631/jzus.A0900208 **Document code:** A **CLC number:** TB6

1 Introduction

The single-stage vapor compression refrigerator operating with pure refrigerants has been widely used in temperature range above −40 °C because of its simple structure and high efficiency. However, in temperature range below −40 °C, serious operation problems will occur in the compressor due to the high pressure ratio across the compressor. Thus, the multi-stage compression refrigerator or cascade refrigerator is usually adapted in these applications, but this complicates the refrigerator.

Two types of single-stage vapor compression refrigerator operating with non-azeotropic mixed refrigerants have been developed for applications from −40 °C down to cryogenic temperature level. One is known as the Linde-Hampson refrigerator (LHR) and the other is auto-cascade refrigerator (ACR) (Gosney, 1982; Gadhiraju and Timmerhaus, 2008). They attracted much attention in recent years for their simple structures and efficiency in comparison with the traditional multi-stage compression refrigerators or cascade refrigerators.

The LHR was originated from the Linde-Hampson liquefier and the early LHR usually ran the open cycle, in which the high pressure pure gas was supplied by a high pressure vessel or a multi-stage compressor. Brodiansky *et al.* (1971) first tried to use mixtures of nitrogen and hydrocarbon for the open

‡ Corresponding author
* Project (Nos. 50876095 and 50890184) supported by the National Natural Science Foundation of China

cycle LHR and they found that the efficiency was improved by a factor of three times in the liquid nitrogen temperature range compared to the case when pure nitrogen was used. Longsworth (1994) first proposed to use mixtures of nitrogen and hydrocarbon for the close cycle LHR in the temperature range 90–130 K with an oil-lubricated single-stage compressor and a high-performance oil separator. Later, much research was conducted on the compositions of the mixture, structures of the heat exchanger and throttle valve to improve the performance by researchers in IGC-APD Cryogenics Inc. (Longsworth, 1997; Boiarski *et al.*, 2000; 2001). Many studies on properties of the mixture and optimization of the single-stage LHR in the temperature range 80–200 K were also conducted by Chinese researchers (Luo *et al.*, 1998; 2004; Gong *et al.*, 2002; 2004a; 2004b; Wang and Chen, 2003), Indian researchers (Ravindranatha *et al.*, 2006; Walimbe *et al.*, 2008) and researchers from other countries (Rozhentsev, 2008; Rozhentsev and Naer, 2009).

The ACR was first announced by Podbielniak (1936). It employs a series of phase separators and recuperators so that some less volatile components will be separated from the main stream before it enters the throttle valve. The heat recuperated in the recuperator will be reduced. In addition, the lubricant oil entrained in the circulating refrigerant mixture can also be effectively removed by the separators to avoid plugging problems in the throttle valve when the temperature is lower than the freezing temperature of the oil. The fundamental difference between the LHR and ACR is that there is no phase separator in the LHR. Thus the circulating mixture composition is uniform in an LHR circuit, while there are more than three different composition mixtures circulating in an ACR circuit. Some research has been conducted to compare the efficiency between the LHR and ACR, but no agreement has been reached as to which cycle has the better efficiency (Boiarski *et al.*, 2001; Alexeev *et al.*, 2003; Gong *et al.*, 2004b). However, it is clear that the LHR possesses a simpler structure than the ACR, but it cannot be used in the applications when the refrigerating temperature level is far lower than the oil's freezing point if no high-performance oil separator is employed due to its inherited deficiency of oil management. Thus the most suitable temperature levels for application of an LHR should be above or a bit below the oil's freezing point, for example, −60 °C for an oil lubricated compressor system.

On the other hand, the binary refrigerant possess the advantage of easy handling in the design, production and maintenance of the refrigerator, especially easy partial recharging after the leak of some refrigerant, compared to the multi-component refrigerant. Therefore, the single-stage LHR operating with binary refrigerant is a promising option for the increasing demands for −60 °C environment in the food industry, medical industry and life sciences nowadays.

To date there are very few reports on the performance optimization of single-stage LHR operating with binary refrigerants at the temperature level of −60 °C. This paper proposes a new approach to optimize the performance of a single-stage LHR operating with six pairs of binary refrigerants based on a semi-analytical model at this temperature level. The optimum compositions and operation conditions obtained in this paper will lay a sound basis for further practical applications.

2 Analyses of a single-stage Linde-Hampson cycle operating with non-azeotropic refrigerants

Fig. 1a shows the flow chart of a single-stage LHR. The non-azeotropic refrigerant partially condenses in the aftercooler and partially evaporates in the evaporator, namely exiting the aftercooler and evaporator in a two-phase region, due to the wide temperature span between the dew point and the bubble point of the refrigerant. Therefore, the discharge pressure and suction pressure, P_2 and P_1, of the compressor are two independent design variables which can be adjusted to some extent to improve the performance of the refrigerator. Fig. 1b shows temperature-entropy (T-s) diagram of the cycle at three different pressure levels.

The pressure ratio is defined as $P_r=P_2/P_1$, which has a strong impact on the volumetric coefficient, polytropic efficiency and discharge temperature of a single-stage compressor. The single-stage compressor is designed to function well in a narrow pressure ratio range, for example, a pressure ratio of 3–5 for high suction pressure compressors (air-conditioning compressors), 6–8 for medium suction pressure compressors, and 9–11 for low suction pressure compressors (refrigerator compressors). Therefore, the pressure ratio was introduced as one of the important design variables in analyzing the performance of a refrigerator operating in three operation conditions shown in Fig. 1b in the following sections.

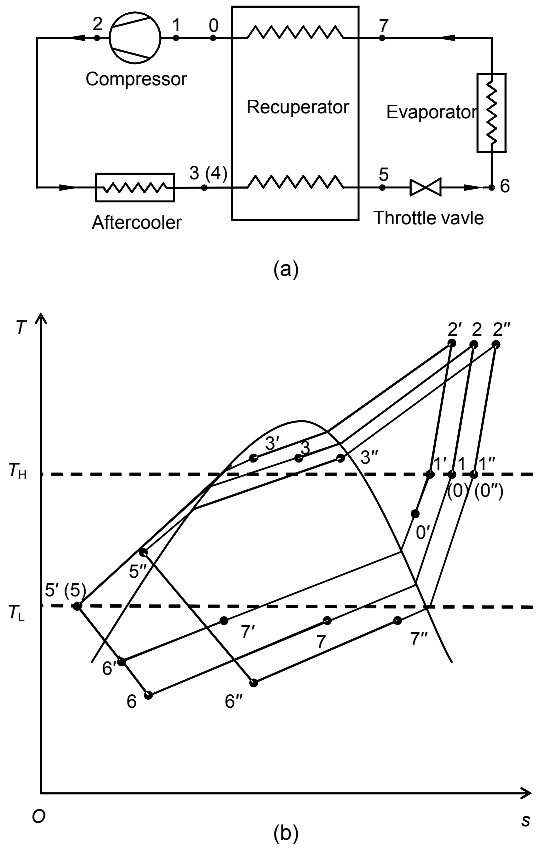

Fig. 1 Flow chart (a) and *T-s* diagram (b) of an LHR
1, 2, …, 7, 1′, 2′, …, 7′, and 1″, 2″, …, 7″ are state points; T_H and T_L are temperatures of heat sink and heat source, respectively

2.1 Assumptions

Analyses will be based on the following assumptions:

(a) The composition of the mixed refrigerant is specified.

(b) The temperatures of heat sink T_H and heat source T_L are specified and isothermal.

(c) The P_r is specified with no pressure loss in the aftercooler, recuperator and evaporator.

(d) The minimum temperature differences in the aftercooler and evaporator are specified as $\Delta T_{A,min}$ and $\Delta T_{E,min}$, which occur at the cold end of the aftercooler and the hot end of the evaporator, respectively.

(e) The minimum temperature difference in the recuperator, $\Delta T_{R,min}$, is specified and $\Delta T_{R,min}=\Delta T_{A,min}=\Delta T_{E,min}$. It occurs at the hot end or the cold end of the recuperator. There is no heat loss in the recuperator.

(f) Total efficiency of the compressor is constant. The suction temperature equals the temperature of the heat sink.

(g) The throttling process is isenthalpic.

2.2 Optimization models

Based on the above assumptions, we can obtain some temperature relationships between state points of the three cycles in Table 1.

Here, the superscripts of single and double quotation marks denote parameters of cycles with the highest and lowest pressure levels, respectively. The pressure level will be represented by the suction pressure P_1 because the pressure ratio has been specified.

Fig. 1 and Table 1 show that the hot refrigerant in the recuperator is sufficiently cooled and the cold refrigerant is sufficiently recuperated in cycle *L* due to the overall matched heat capacity rates of the hot and

Table 1 Temperature relationships between state points

Cycle L'	Cycle L	Cycle L''
$1'\to2'\to3'\to5'\to6'\to7'\to0'\to1'$	$1\to2\to3\to5\to6\to7\to0\to1$	$1''\to2''\to3''\to5''\to6''\to7''\to0''\to1''$
$T_{1'}=T_H$	$T_1=T_H$	$T_{1''}=T_H$
$T_{3'}=T_H+\Delta T_{A,min}$	$T_3=T_H+\Delta T_{A,min}$	$T_{3''}=T_H+\Delta T_{A,min}$
$T_{0'}<T_3-\Delta T_{R,min}=T_H$	$T_0=T_3-\Delta T_{R,min}=T_H$	$T_{0''}=T_3-\Delta T_{R,min}=T_H$
$T_{7'}=T_L-\Delta T_{E,min}=T_7$	$T_7=T_L-\Delta T_{E,min}$	$T_{7''}=T_L-\Delta T_{E,min}=T_7$
$T_{5'}=T_{7'}+\Delta T_{R,min}=T_L$	$T_5=T_7+\Delta T_{R,min}=T_L$	$T_{5''}=T_{7''}+\Delta T_{R,min}>T_L$

cold refrigerants. But the cold refrigerant is not recuperated sufficiently in cycle L' and the hot refrigerant is not cooled sufficiently in cycle L'' due to the mismatched heat capacity rates of the hot and cold refrigerants in both cycles. Thus, the pinch points occur at the cold and hot ends of the recuperator in cycle L' and cycle L'', respectively. Only in cycle L, the pinch point occurs at the cold and hot ends of the recuperator at the same time.

When the pressure level is very low, the quality of the low pressure mixed refrigerant at the outlet of the evaporator is great. We can see the case of cycle L'' in Fig. 1b. The heat capacity rate of the low pressure mixed refrigerant is not large enough to cool the high pressure mixed refrigerant. Thus $T_{0''}$ will increases until it becomes equal to the ambient temperature T_H while the high pressure mixed refrigerant will not be cooled down to T_5, namely, $T_{5''}>T_L$. The pinch point occurs at the hot end of the recuperator, namely, $\Delta T_{R,hot}=T_{3''}-T_{0''}=\Delta T_{R,min}$.

When the pressure level increases, the quality of the low pressure mixed refrigerant at the outlet of the evaporator lessens. The low pressure mixed refrigerant will provide a larger heat capacity rate to cool the high pressure mixed refrigerant, and $T_{5''}$ will decrease at the same time. When the pressure level is high enough, the overall heat capacity rate of the low pressure mixed refrigerant matches that of the high pressure mixed refrigerants. Namely, $\Delta T_{R,hot}=T_3-T_0=\Delta T_{R,min}$ and $\Delta T_{R,cold}=T_5-T_7=\Delta T_{R,min}$. We can see the case of cycle L in Fig. 1b.

When the pressure level is higher than that of cycle L, the heat capacity rate of the low pressure mixed refrigerant will be too much for cooling the high pressure mixed refrigerant due to the low quality of the low pressure mixed refrigerant at the outlet of the evaporator (as the latent heats of vaporization of almost all pure substances decrease when the saturated pressure increases, the mixed refrigerants should also follow this using basic thermodynamics). We can see the case of cycle L' in Fig. 1b. Therefore, $T_{0'}$ will be lower than the ambient temperature T_H while the high pressure mixed refrigerant will be cooled down easily to $T_{5'}=T_5$ due to its relatively small heat capacity rate. Hence the pinch point occurs at the cold end of the recuperator, namely, $\Delta T_{R,cold}=T_5-T_{7'}=\Delta T_{R,min}$ and $T_{0'}<T_H$. Because $\Delta T_{E,min}=T_L-T_{7'}$ and $\Delta T_{R,min}=\Delta T_{E,min}$, from these assumptions, we can deduce $T_{5'}=T_5=T_L$.

In conclusion, the pinch point will shift from the hot end of the recuperator to the cold end of the recuperator as the pressure level increases.

Combined with the heat balance in the recuperator, coefficients of performance (COPs) of these cycles can be expressed as follows:

$$\begin{aligned}\mathrm{COP}' &= q'_E / w'_p = (h_{7'} - h_{5'}) / (h_{2'} - h_{1'}) \\ &= (h_{0'} - h_{3'}) / (h_{2'} - h_{1'}),\end{aligned} \tag{1}$$

$$\begin{aligned}\mathrm{COP} &= q_E / w_p = (h_7 - h_5) / (h_2 - h_1) \\ &= (h_0 - h_3) / (h_2 - h_1),\end{aligned} \tag{2}$$

$$\begin{aligned}\mathrm{COP}'' &= q''_E / w''_p = (h_{7''} - h_{5''}) / (h_{2''} - h_{1''}) \\ &= (h_{0''} - h_{3''}) / (h_{2''} - h_{1''}),\end{aligned} \tag{3}$$

where q_E is the specific refrigerating effect, kJ/kmol, w_p is the specific work of polytropic compression, kJ/kmol, and h is the specific enthalpy of the refrigerant, kJ/kmol.

The specific work consumption of cycle L can also be expressed as (Reynolds, 1977)

$$\begin{aligned}w_p &= \frac{w_s}{\xi_C} = \frac{n_s}{n_s - 1}\frac{Z_1 R T_1}{\xi_C}\left(1 - \left(\frac{P_2}{P_1}\right)^{\frac{n_s - 1}{n_s}}\right) \\ &= \frac{n_s}{n_s - 1}\frac{Z_1 R T_1}{\xi_C}\left(1 - P_r^{\frac{n_s - 1}{n_s}}\right),\end{aligned} \tag{4}$$

where w_s is the specific work of isentropic compression, kJ/kmol, ξ_C is the total efficiency of the compressor, n_s is the isentropic exponent, Z_1 is the compressibility factor of the refrigerant at state point 1, and R is the gas constant, kJ/(kmol·K).

From the above assumptions, P_r, T_1 and ξ_C remain constant for the three cycles. On the other hand, n_s and Z_1 are approximately constant if only P_1 varies a little. Therefore, from Eq. (4) the specific work consumption of the three cycles is found to be approximately equal:

$$w'_p \approx w_p \approx w''_p. \tag{5}$$

Combining Eqs. (4) and (5), we can find that COPs of these cycles are almost determined by their specific refrigerating effects. Thus, we can analyze the impact of the pressure level on the cycle COP by way of the specific refrigerating effect of the cycle.

When the pressure level moves from cycle L'' to L, the pinch point is at the hot end of the recuperator. $h_{3''}$ decreases greatly because the quality of the mixed refrigerant at point 3″ decreases due to the increased P_1 (usually the point 3″ is within the two-phase region due to the large temperature glide of the mixed refrigerant). But $h_{0''}$ decreases only a little since $T_{1''}$ remains constant. Namely, $h_{3''}$ decreases more than $h_{0''}$ when P_1 increases. Therefore, $(h_{0''}-h_{3''})$ increases when P_1 increases. Thus from Eq. (1), it can be found that COP″ increases until the pressure level is equal to cycle L. At this pressure level, COP″ equals to COP and temperature differences at both ends of the recuperator are equal to the minimum temperature difference, i.e., $\Delta T_{\rm R,hot}=T_3-T_0=\Delta T_{\rm R,cold}=T_5-T_7=\Delta T_{\rm R,min}$.

When the pressure level moves from cycle L to cycle L', the pinch point is shifted to the cold end of the recuperator. Thus $T_{5'}$ remains constant, $T_{5'}=T_5$, and $h_{5'}\approx h_5$. As the enthalpy of the subcooled mixed refrigerant liquid at point 5, $h_{5'}=h(P_{5'},T_{5'})$ varies slightly with the pressure using basic thermodynamics. $h_{7'}$ decreases obviously with the increased P_1 since point 7 is within the two-phase region (due to the larger heat capacity rate of the low pressure mixed refrigerant). Namely, $h_{7'}$ decreases at a greater rate than $h_{5'}$ when P_1 increases. Therefore, $(h_{7'}-h_{5'})$ decreases when P_1 increases. Thus, from Eq. (3), it can be found that COP′ decreases when the pressure level departs from cycle L to cycle L'.

Based on the above discussion and many calculations for different working mixture components and temperature levels, it was found that the maximum COP occurs at the pressure level of cycle L, in which the heat capacity rates of the hot and cold refrigerants are overall matched. Therefore, we can take advantage of this characteristic to simplify the optimization process of an LHR. At a specified mixture composition and operating pressure ratio, only mixture properties of four state points 3, 0, 5, 7 have to be calculated to compare $\Delta T_{\rm R,hot}$, $\Delta T_{\rm R,cold}$ and $\Delta T_{\rm R,min}$ to search for the optimum pressure level. It is unnecessary to calculate mixture properties of all points and performance of the cycle until the optimum pressure level is obtained. Thus calculation time is greatly reduced.

Similarly, optimizations of the pressure level can be performed for different interested mixture compositions and pressure ratios. Therefore, the optimum composition, optimum pressure ratio based on COPs at corresponding optimum pressure levels can be obtained as well as a regular pattern of COPs.

2.3 Exergy analysis models

To further analyze the available work lost in each process on cycle COP, exergy analyses will be performed based on the second law of thermodynamics. The exergy efficiency is defined as

$$\eta_{\rm e}=\frac{\rm COP}{{\rm COP}_{\rm Carnot}}=\frac{w_{\rm Carnot}}{w_{\rm p}}=1-\frac{\sum w_{{\rm lost},i}}{w_{\rm p}}=1-\sum\beta_i, \quad (6)$$

where the subscript "Carnot" denotes the Carnot cycle, $w_{{\rm lost},i}$ is the specific exergy loss in process i, kJ/kmol, and β_i is the exergy loss ratio in process i. Eqs. (7)–(11) are formulas to calculate β_i, respectively, which can be derived from the Gouy-Stodola theorem and the second law for a control volume (Bejan, 1997).

$$\beta_{\rm C}=T_{\rm H}s_{\rm g,C}/w_{\rm p}=T_{\rm H}(s_2-s_1)/w_{\rm p}+f_{\rm C}, \quad (7)$$

$$\beta_{\rm A}=T_{\rm H}s_{\rm g,A}/w_{\rm p}=[(h_2-h_3)-T_{\rm H}(s_2-s_3)]/w_{\rm p}, \quad (8)$$

$$\beta_{\rm T}=T_{\rm H}s_{\rm g,C}/w_{\rm p}=T_{\rm H}(s_6-s_5)/w_{\rm p}, \quad (9)$$

$$\beta_{\rm E}=T_{\rm H}s_{\rm g,E}/w_{\rm p}=T_{\rm H}[(s_7-s_6)-(h_7-h_6)]/w_{\rm p}, \quad (10)$$

$$\beta_{\rm R}=T_{\rm H}s_{\rm g,R}/w_{\rm p}=T_{\rm H}[(s_0-s_7)-(s_3-s_5)]/w_{\rm p}, \quad (11)$$

where the subscripts "C", "A", "T", "E" and "R" denote the processes in the compressor, aftercooler, throttle valve, evaporator and recuperator, respectively, s is the specific entropy of the refrigerant, kJ/(kmol·K), $s_{\rm g}$ is the specific entropy production, kJ/(kmol·K), and $f_{\rm C}$ is the ratio of the specific heat dissipated from the compressor to the specific work of the compressor.

Eq. (11) can be transformed as

$$\beta_{\rm R}=T_{\rm H}(s_{\rm g,R}/q_{\rm R})(q_{\rm R}/w_{\rm p})=T_{\rm H}y_{\rm g,R}f_{\rm R}, \quad (12)$$

where q_R is the specific heat recuperated, kJ/kmol, $y_{g,R}$ is the entropy production per unit heat recuperated, K^{-1}, and f_R is the ratio of the specific heat recuperated to the specific work of the compressor.

$y_{g,R}$ and f_R are two useful independent parameters to analyze the exergy loss ratio in the recuperator, β_R. $y_{g,R}$ represents the irreversibility per unit heat recuperated in the recuperating process and is determined only by the temperature differences of the hot and cold refrigerants in the recuperator, namely by the local match of heat capacity rates of the refrigerants. f_R depends not only on the heat recuperated but also on the work consumption of the compressor.

3 Simulations of a single-stage Linde-Hampson cycle operating with binary refrigerants

Two volatile pure refrigerants R23, R170 and six less volatile pure refrigerants R134a, R227ea, R236ea, R290, R600a and R600 were selected. Physical and environmental data of these pure refrigerants are listed in Table 2 (Desmarteau and Beyerlein, 1996; IPPC, 2000; Calm and Hourahan, 2007).

Table 2 Physical and environmental data of eight pure refrigerants

Refrigerant	NBP (°C)	LFL (%, v/v)	ODP	GWP
R23	−82.1	None	0	12000
R134a	−26.1	None	0	1300
R227ea	−15.6	None	0	3500
R236ea	6.5	None	0	1200
R170	−88.9	2.9	0	~20
R290	−42.2	2.1	0	~20
R600a	−11.7	1.7	0	~20
R600	−0.5	1.5	0	~20

NBP: normal boiling point; LFL: lower flammability limit; ODP: ozone depletion potential; GWP: global warming potential

These pure refrigerants were coupled in six pairs of binary refrigerants, which can be divided in two groups as follows:

(a) R23/R134a, R23/R227ea, R23/R236ea;

(b) R170/R290, R170/R600a, R170/R600.

From Table 2, it can be found that each of the above binary refrigerants has an ODP of zero. The three R23 based binary refrigerants in group (a) consist of fluorinated hydrocarbons and are all nonflammable, but each has a very large GWP. The three R170 based binary refrigerants in group (b) consist of hydrocarbons and all have very small GWP, but all flammable.

Following the signing of the 1987 Montreal Protocol, it became important to replace chlorofluorocarbons (CFCs) with alternatives having ozone depletion potentials (ODPs) of zero (Missimer, 1997) in the old systems and to use mixed refrigerants with ODPs of zero in new systems. Nonflammable mixed refrigerants are also greatly concerned in many applications (Boiarski *et al.*, 2005; Khatri and Boiarski, 2008). It would appear that, to date, there is no good solution for LHR or ACR for selecting efficient nonflammable mixed refrigerants with ODPs of zero and low GWPs.

Based on the optimization models and exergy analysis models presented in Section 2, performances of an LHR operating with these binary refrigerants were simulated at three pressure ratios of 4, 7, 10 and the following operation conditions: T_H=26.85 °C, T_L=−60°C, $\Delta T_{R,min}$=$\Delta T_{H,min}$=$\Delta T_{L,min}$=2 °C, ξ_C=0.4, f_C=0.4. The thermodynamic properties of binary refrigerants required in cycle simulations were supplied by REFPROP routines (NIST, 2007).

3.1 Optimization of pressure levels

Optimization of pressure levels was performed at a specified mole fraction of each pair of components at a specified pressure ratio using the method described in Section 2. Fig. 2 gives six typical variations of COP, $\Delta T_{R,hot}$ and $\Delta T_{R,cold}$ with the suction pressures at a P_r of 7, where z was the mole fraction of the volatile component of the binary refrigerant.

Fig. 2 shows that the optimum COP occurs at the suction pressure when $\Delta T_{R,hot}$ and $\Delta T_{R,cold}$ minimize and approximately equal $\Delta T_{R,min}$ at the same time in each case. It indicates that the optimum COP occurs at the pressure level when the heat capacity rates of the hot and cold fluids are overall matched. These numerical calculation results verify the analytical results in Section 2. Fig. 2 also shows that variations of COP with P_1 differ greatly for these six binary

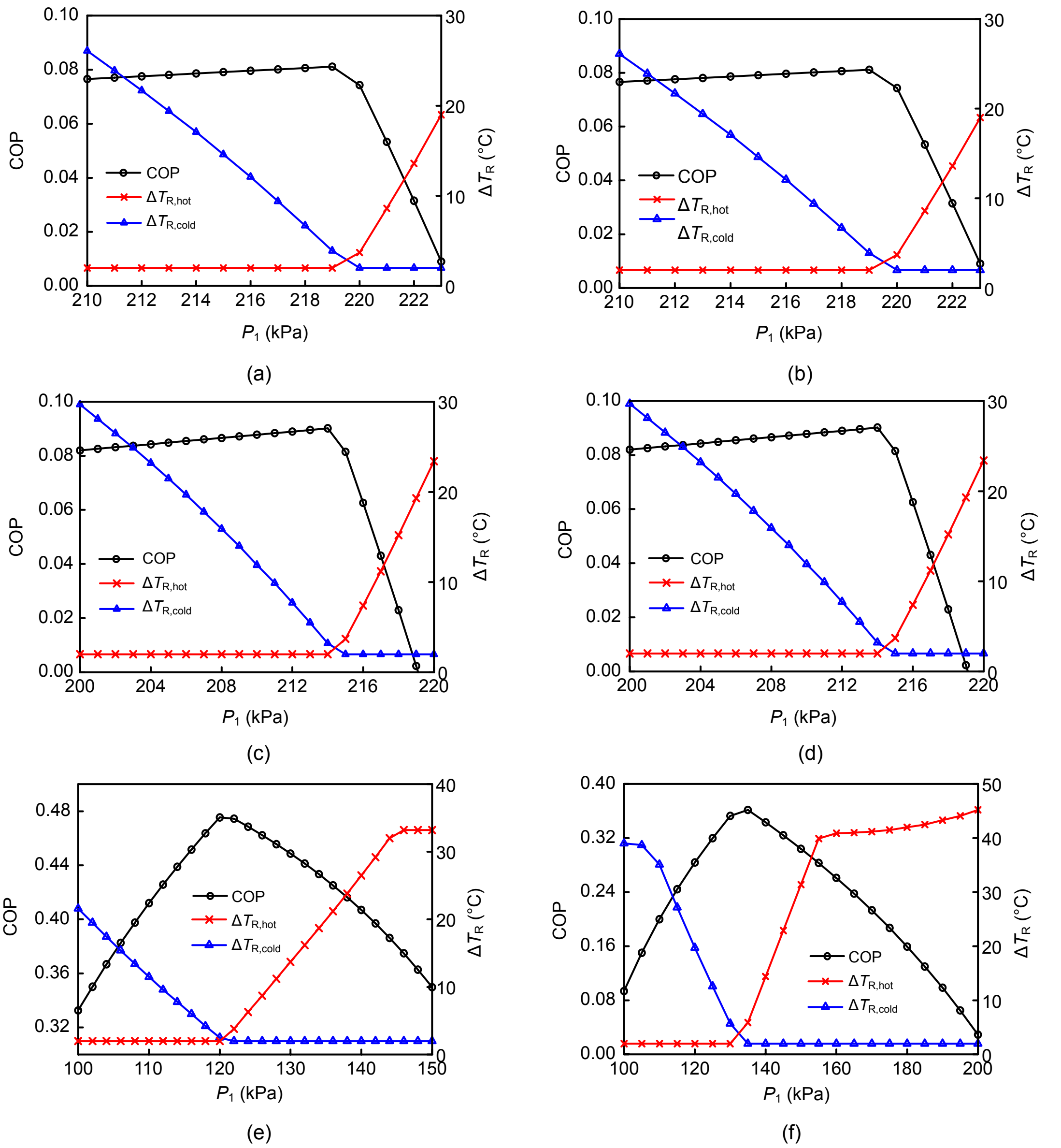

Fig. 2 Variations of COP, $\Delta T_{R,hot}$ and $\Delta T_{R,cold}$ with the suction pressure P_r=7
(a) R23/R134a (z=0.8); (b) R170/R290 (z=0.8); (c) R23/R227ea (z=0.8); (d) R170/R600a (z=0.6); (e) R23/R236ea (z=0.55); (f) R170/R600 (z=0.6)

refrigerants. Most COPs vary sharply near the optimum P_1. It suggests that it is necessary to optimize the pressure level for a specified mole fraction of the binary refrigerant before the optimization of its mole fraction. The result will not be significant if the optimization of the mole fraction is conducted at the same fixed pressure level.

The COPs at an optimum pressure level, COP_{opt}, were calculated in a mole fraction range of z=0.4−0.8 and P_r of 4, 7, and 10 for the six pairs of binary components. The results were presented in Fig. 3.

3.2 Optimization of compositions

3.2.1 Optimization of mole fractions

Fig. 3 shows that variations of COP_{opt} with the mole fraction for different P_r can be divided into two types. One is a monotonic increasing type and the other is a peak type. The variation type is determined not only by P_r but also by the kind of components, especially on the normal boiling temperature difference between two components. For example, COP_{opt} for R23/R134a, R170/R290 and R23/R227ea

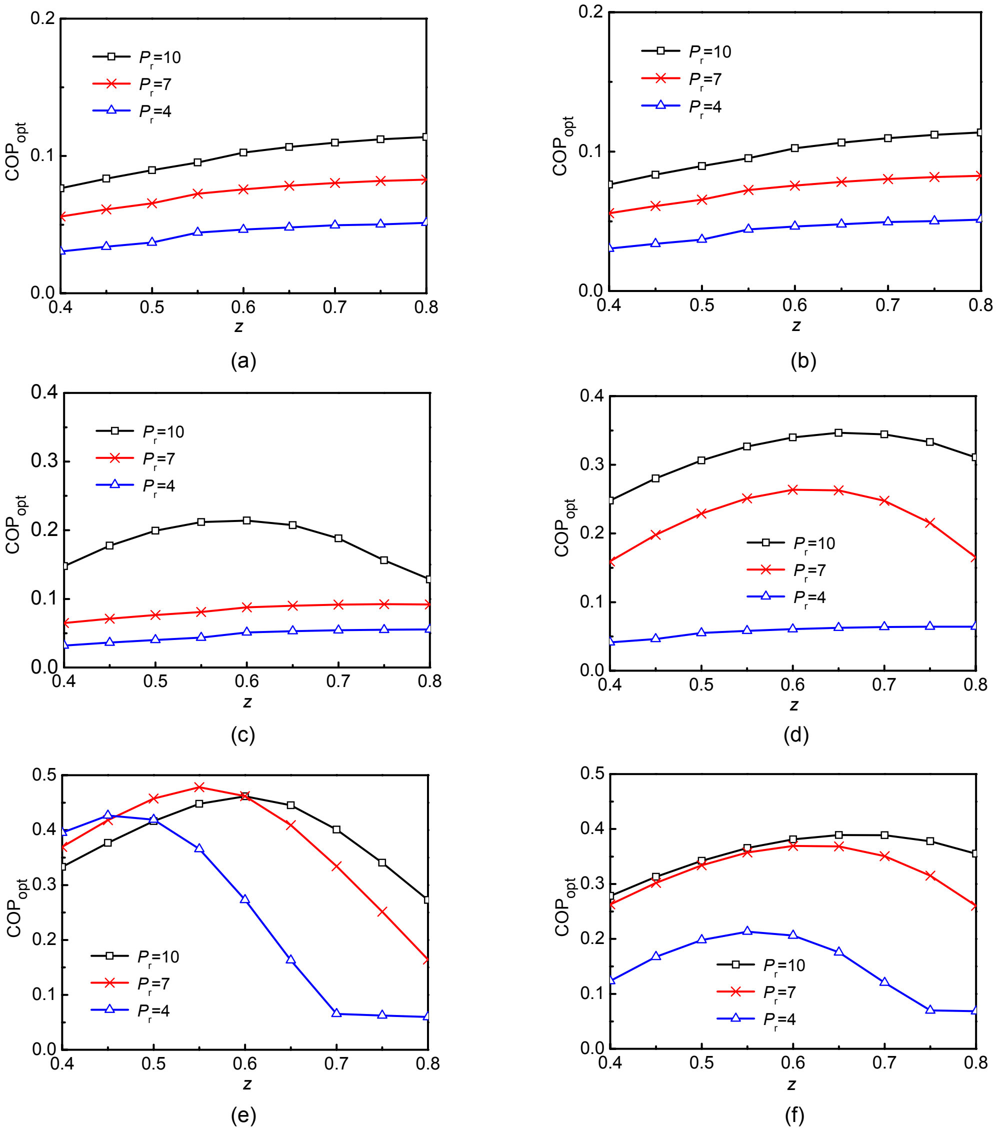

Fig. 3 Variations of COP_{opt} with the mole fraction and pressure ratio

(a) R23/R134a; (b) R170/R290; (c) R23/R227ea; (d) R170/R600a; (e) R23/R236ea; (f) R170/R600

belong to a monotonic increasing type but COP_{opt} for R170/R600a, R23/R236ea, R170/R600 belong to a peak type at P_r=7. Table 3 gives the results of exergy analysis for an LHR operating with six pairs of binary refrigerants at mole fractions of z=0.4, 0.6, 0.8 and a P_r of 7.

Table 3 shows that differences of the exergy loss ratios in the expansion valve and evaporator, β_T and β_L, between different mole fractions were all much smaller when compared with those in the compressor, condenser and recuperator, β_C, β_H and β_R. When z increases for each pair of components, β_C increases while β_H decreases. β_R monotonously decreases for R23/R134a, R170/R290 and R23/R227ea, but valley points occur for R170/R600a, R23/R236ea, R170/R600 corresponding to the variation type of COP_{opt}. It indicates that the variation type of β_R determines the variation type of COP_{opt}.

Table 3 also shows that f_R decreases as z increases for each pair of components, but $y_{g,R}$ monotonously increases for R23/R134a, R170/R290 and R23/R227ea, but valley points occur for R170/R600a,

Table 3 An example of exergy analysis results on influences of the mole fraction (P_r=7)

Parameter	R23/R134a			R170/R290		
	z=0.40	z=0.60	z=0.80	z=0.40	z=0.60	z=0.80
P_1 (kPa)	111.75	164.14	219.59	140.46	201.46	270.29
COP_{opt}	0.0559	0.0756	0.0827	0.0556	0.0777	0.0923
η_e	0.0228	0.0308	0.0337	0.0227	0.0317	0.0376
β_C	0.5523	0.5520	0.5473	0.5501	0.5501	0.5471
β_H	0.0959	0.1063	0.1174	0.1023	0.1110	0.1198
β_T	0.0046	0.0062	0.0076	0.0061	0.0084	0.0106
β_L	0.0011	0.0013	0.0013	0.0011	0.0014	0.0015
β_R	0.3233	0.3034	0.2927	0.3177	0.2974	0.2834
$y_{g,R}$ (1/K)	5.544E−04	5.792E−04	6.283E−04	6.498E−04	6.632E−04	6.957E−04
f_R	1.9440	1.7458	1.5530	1.6297	1.4949	1.3580
Parameter	R23/R227ea			R170/R600a		
	z=0.40	z=0.60	z=0.80	z=0.40	z=0.60	z=0.80
P_1 (kPa)	102.23	155.04	214.44	94.98	154.83	257.91
COP_{opt}	0.0648	0.0877	0.0918	0.1592	0.2637	0.1651
η_e	0.0264	0.0357	0.0374	0.0649	0.1074	0.0673
β_C	0.5630	0.5613	0.5533	0.5569	0.5554	0.5501
β_H	0.0730	0.0872	0.1049	0.0879	0.1020	0.1152
β_T	0.0058	0.0075	0.0086	0.0061	0.0084	0.0109
β_L	0.0014	0.0016	0.0015	0.0056	0.0091	0.0030
β_R	0.3304	0.3067	0.2943	0.2786	0.2177	0.2535
$y_{g,R}$ (1/K)	4.897E−04	5.241E−04	5.925E−04	5.076E−04	4.792E−04	6.066E−04
f_R	2.2493	1.9502	1.6558	1.8295	1.5146	1.3929
Parameter	R23/R236ea			R170/R600		
	z=0.40	z=0.60	z=0.80	z=0.40	z=0.60	z=0.80
P_1 (kPa)	67.21	146.50	219.73	71.55	132.89	250.12
COP_{opt}	0.3694	0.4618	0.1644	0.2629	0.3692	0.2604
η_e	0.1505	0.1882	0.0670	0.1071	0.1504	0.1061
β_C	0.5627	0.5568	0.5523	0.5578	0.5532	0.5501
β_H	0.0777	0.1024	0.1086	0.0871	0.1048	0.1179
β_T	0.0156	0.0080	0.0086	0.0086	0.0090	0.0106
β_L	0.0321	0.0166	0.0027	0.0154	0.0188	0.0056
β_R	0.1614	0.1280	0.2608	0.2240	0.1638	0.2097
$y_{g,R}$ (1/K)	2.629E−04	2.607E−04	5.404E−04	4.146E−04	3.750E−04	5.280E−04
f_R	2.0464	1.6360	1.6086	1.8008	1.4559	1.3239

R23/R236ea, R170/R600. It indicates that the variation type of $y_{g,R}$ determines the variation types of β_R and COP_{opt}.

The above analysis reveals that it is necessary to optimize mole fractions of the refrigerants before comparing COPs of an LHR operating with different component refrigerants. If the comparison is conducted at the same fixed mole fractions the result will not be significant.

Comparing COP_{opt} in Fig. 3, the maximum COP for each pair of components at each specified P_r, COP_{max}, can be selected. Table 4 gives the results of selection and exergy analyses on an LHR operating with binary refrigerants at three pressure ratios.

Table 4 COP_{max} and exergy analyses for six pairs of components at three P_r

Parameter	R23/R134a			R170/R290		
	P_r=4	P_r=7	P_r=10	P_r=4	P_r=7	P_r=10
z	0.80	0.80	0.80	0.80	0.80	0.80
P_1 (kPa)	221.88	219.59	216.72	273.77	270.29	265.54
COP_{max}	0.0513	0.0827	0.1138	0.0557	0.0923	0.1318
η_e	0.0209	0.0337	0.0464	0.0227	0.0376	0.0537
β_C	0.5612	0.5414	0.5346	0.5602	0.5471	0.5397
β_H	0.0851	0.0959	0.1174	0.0867	0.1198	0.1420
β_T	0.0056	0.0046	0.0076	0.0078	0.0106	0.0130
β_L	0.0008	0.0011	0.0013	0.0009	0.0015	0.0023
β_R	0.3264	0.3233	0.2927	0.3217	0.2834	0.2493
$y_{g,R}$ (1/K)	4.677E−04	5.544E−04	6.283E−04	5.232E−04	6.957E−04	7.779E−04
f_R	2.3267	1.9440	1.5530	2.0492	1.3580	1.0685
Parameter	R23/R227ea			R170/R600a		
	P_r=4	P_r=7	P_r=10	P_r=4	P_r=7	P_r=10
z	0.80	0.80	0.60	0.80	0.60	0.65
P_1 (kPa)	217.30	214.44	136.89	269.33	154.83	150.00
COP_{max}	0.0554	0.0918	0.2142	0.0643	0.2637	0.3465
η_e	0.0226	0.0374	0.0873	0.0262	0.1074	0.1412
β_C	0.5660	0.5533	0.5521	0.5630	0.5554	0.5475
β_H	0.0751	0.1049	0.1038	0.0822	0.1020	0.1253
β_T	0.0063	0.0086	0.0087	0.0082	0.0084	0.0106
β_L	0.0009	0.0015	0.0057	0.0010	0.0091	0.0167
β_R	0.3291	0.2943	0.2424	0.3194	0.2177	0.1587
$y_{g,R}$ (1/K)	4.446E−04	5.925E−04	5.466E−04	4.894E−04	4.792E−04	4.948E−04
f_R	2.4678	1.6558	1.4783	2.1754	1.5146	1.0690
Parameter	R23/R236ea			R170/R600		
	P_r=4	P_r=7	P_r=10	P_r=4	P_r=7	P_r=10
z	0.45	0.55	0.60	0.55	0.60	0.65
P_1 (kPa)	127.36	120.73	121.32	162.05	132.89	129.32
COP_{max}	0.4269	0.478	0.4617	0.2133	0.3692	0.3891
η_e	0.1739	0.1948	0.1881	0.0869	0.1504	0.1585
β_C	0.5696	0.5584	0.5512	0.5684	0.5532	0.5458
β_H	0.0626	0.0971	0.1199	0.0719	0.1048	0.1279
β_T	0.0069	0.0087	0.0098	0.0062	0.0090	0.0108
β_L	0.0156	0.0247	0.0259	0.0055	0.0188	0.0245
β_R	0.1714	0.1163	0.1051	0.2611	0.1638	0.1325
$y_{g,R}$ (1/K)	1.939E−04	2.283E−04	2.741E−04	3.445E−04	3.750E−04	4.121E−04
f_R	2.9467	1.6976	1.2788	2.5263	1.4559	1.0715

3.2.2 Optimization of components

Table 4 shows that COP_{max} for R23/R236ea and R170/R600 are the largest at all pressure ratios among COP_{max} for the components listed in groups (a) and (b), respectively, while COP_{max} for R23/R134a and R170/R290 are the smallest. It indicates that the boiling temperature difference of two components is an important guide for the selection of refrigerant components. By comparing the exergy loss ratios of all processes, we find that the improvement of COP_{max} fundamentally benefits from the reduction of β_R at a specified P_r, especially from the reduction of $y_{g,R}$, which can be described more clearly with the temperature distributions of hot and cold refrigerants in the recuperator. For example, Fig. 4 gives the recuperator temperature profiles of the six binary refrigerants listed in Table 4 at P_r=7.

Fig. 4 shows that the pinch points all occur at the hot and cold ends of the recuperator for six binary refrigerants, which indicates that the heat capacity rates of hot and cold refrigerants in the recuperator are matched overall at the optimized pressure level. However, the average temperature difference between hot and cold refrigerants in the recuperator for R23/R236ea, which can be represented by the area down to the horizontal ordinate under the temperature difference profile, is much smaller than those of R23/R227ea and R23/R134a. Similar relationships of the average temperature difference can also be observed for R170/R600, R170/R600a and R170/R290 from Fig. 4. It clearly shows that not only the overall match of heat capacity rates in the recuperator is necessary for the improvement of COP, but the local match which can be improved by the component selection and the mole fraction optimization is also

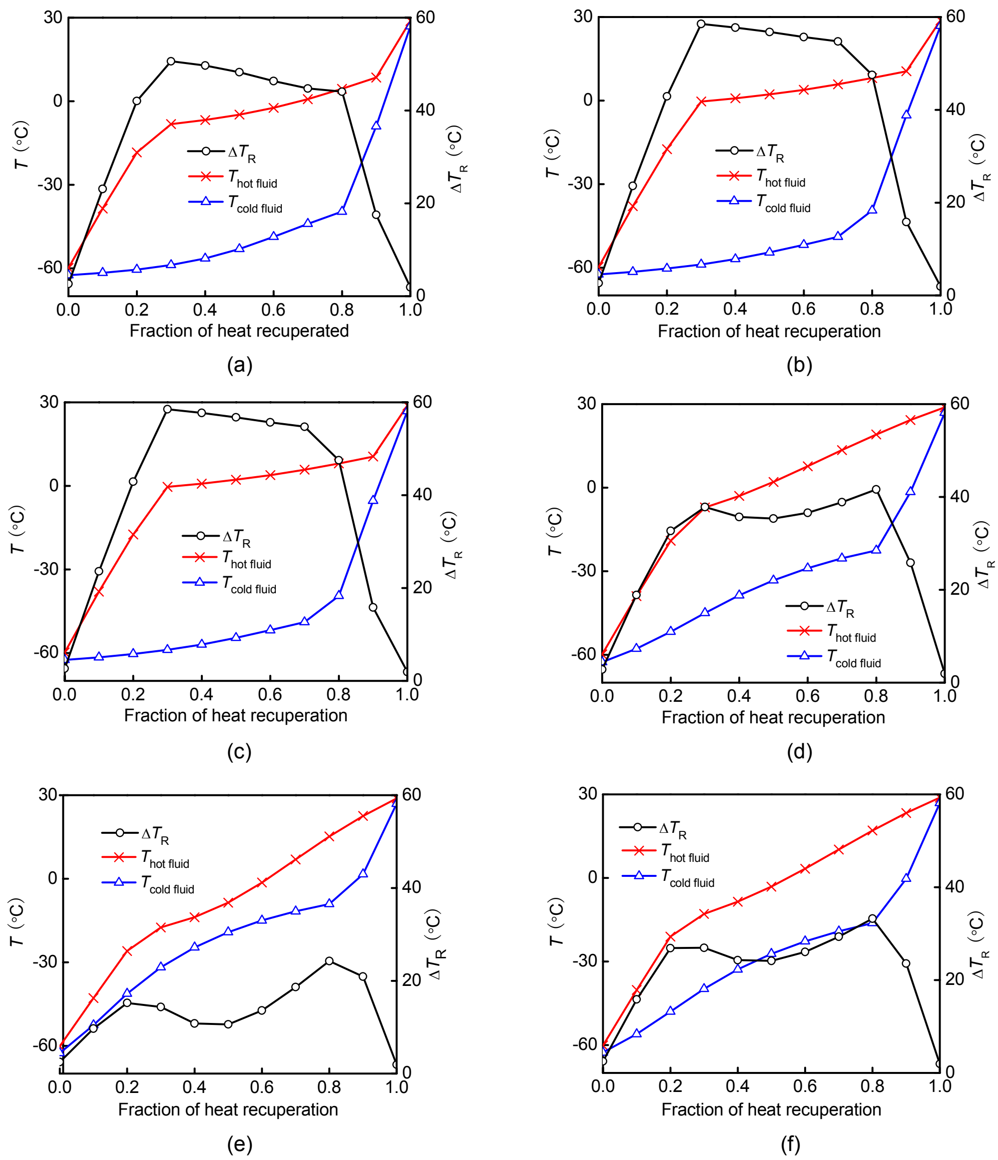

Fig. 4 Recuperator temperature profiles for six binary refrigerants

(a) R23/R134a (z=0.8, P_r=7); (b) R170/R290 (z=0.8, P_r=7); (c) R23/R227ea (z=0.8, P_r=7); (d) R170/R600a (z=0.6, P_r=7); (e) R23/R236ea (z=0.55, P_r=7); (f) R170/R600 (z=0.6, P_r=7) very important. Table 4 shows that R23/R236ea and R170/R600 are the best components in groups (a) and (b) at the specified three pressure ratios, respectively.

3.2.3 Optimization of pressure ratios

Comparing COP_{max} for the same component refrigerants at different P_r in Table 4, it can be found that COP_{max} increases as P_r increases except for R23/R236ea. It can also be found that variations of β_T and β_E are all much smaller than those of β_C, β_A and β_R. β_C and β_R decrease while β_A increases as P_r increases. The improvement of COP_{max} is attributed to the reduction of β_R, especially the reduction of f_R when P_r increases from 7 to 10 except in the case of R23/R236ea. It can be explained that some heat capacity rates of the recuperator shift to the condenser due to the decrease of the quality of the refrigerant at state point 3 when P_r increases, which results in a reduction of β_R and an increase of β_A. If the reduction of β_R is larger than the increase of β_H, the COP_{max} will increase; otherwise, the COP_{max} will decrease.

Table 4 also shows that the suction pressures for optimum compositions of the candidate refrigerants are too low at P_r=4, which indicates that high suction pressure compressors (air-conditioning compressors) are not the correct choice for the single-stage LHR operating with binary refrigerants at the temperature level of −60 °C. R23/R227ea with mole fractions of 0.55 and 0.6 should be the most promising nonflammable refrigerant compositions in group (a) for medium and low suction pressure compressors (P_r=7 and P_r=10), respectively. R170/R600a with mole fractions of 0.6 and 0.65 should be the most promising compositions of refrigerants with low GWPs in group (b) for medium and low suction pressure compressors (P_r=7 and P_r=10), respectively.

4 Conclusion

Based on the above discussions, the following conclusions can be derived:

(1) The performance of a single-stage LHR operating with non-azeotropic mixed refrigerant is determined by the refrigerant composition (component and mole fraction) and operation pressure condition (pressure level and pressure ratio); therefore, it is necessary to optimize mole fractions of the refrigerants respectively based on corresponding optimized operating pressure levels before comparing COPs for different component refrigerants.

(2) The optimum suction pressure for COP occurs when $\Delta T_{R,hot}$ and $\Delta T_{R,cold}$ are approximately equal to $\Delta T_{R,min}$ in the recuperator at a specified composition and pressure ratio; namely, the heat capacity rates of the hot and cold refrigerants reach an overall match in the recuperator.

(3) The variation of COP_{opt} with the mole fraction can be divided into the monotonic increasing type and the peak type at a specified pressure ratio, which is fundamentally determined by the variation type of the $y_{g,R}$.

(4) Air-conditioning compressors are not suitable for the single-stage LHRs operating with binary refrigerants at the temperature level of −60 °C. The 0.55 and the 0.6 mole fractions of R23 for R23/R236ea are the most prospective nonflammable refrigerants in group (a) for medium and low suction pressure compressors, respectively. The 0.6 and the 0.65 mole fractions of R170 for R170/R600 are the most prospective refrigerants with low GWPs in group (b) for these two kinds of compressors, respectively. The improvement of COP_{max} primarily benefits from the reduction of β_R at a specified P_r, especially from the reduction of $y_{g,R}$.

The new approach employed in this paper also suggests a promising application even to the optimization of the performance with multi-component refrigerants.

References

Alexeev, A., Goloubev, D., Mantwill, E., 2003. Efficiency of the ARC and mixed gas Joule-Thomson refrigerators. *Cryocoolers*, **12**:595-601.

Bejan, A., 1997. Advanced Engineering Thermodynamics. John Wiley & Sons, Inc., USA, p.109-111.

Boiarski, M., Khatri, A., Podtcherniaev, O., 2000. Enhanced refrigeration performance of the throttle-cycle coolers operating with mixed refrigerants. *Advances in Cryogenic*, **45**:291-297.

Boiarski, M., Khatri, A., Podtcherniaev, O., Kovalenko, V., 2001. Modern trends in designing small-scale throttle-cycle coolers operating with mixed refrigerants. *Cryocoolers*, **11**:513-521.

Boiarski, M., Podtcherniaev, O., Flynn, K., 2005. Comparative performance of throttle cycle cryotiger coolers operating with different mixed refrigerants. *Cryocoolers*, **13**:481-488.

Brodiansky, V.M., Gresin, A.K., Gromov, E.M., Yagoden, V.M., Nicolaky, V.N., Alpheev, V.N., 1971. The Use of Mixtures as Working Gas in Throttle (J-T) Cryogenic Refrigerators. Proceedings 13th International Congress of Refrigeration, Washington DC, USA, **1**:43-46.

Calm, J.M., Hourahan, G.C., 2007. Refrigerant data update. *Heating/Piping/Air Conditioning Engineering*, **79**(1): 50-64.

Desmarteau, D.D., Beyerlein, A.L., 1996. New Chemical Alternatives for the Protection of Stratospheric Ozone. EPA Project Summary, EPA/600/SR-95/113, National Risk Management Research Laboratory, Cincinnati, USA.

Gadhiraju, V., Timmerhaus, K.D., 2008. Cryogenic Mixed Refrigerant Processes. Springer, NewYork, USA.

Gong, M.Q., Luo, E.C., Wu, J.F., Zhou, Y., 2002. On the temperature distribution in the counter flow heat exchanger with multicomponent non-azeotropic mixtures. *Cryogenics*, **42**(12):795-804. [doi:10.1016/S0011-2275(02)00148-0]

Gong, M.Q., Luo, E.C., Wu, J.F., 2004a. Performances of the mixed-gases Joule-Thomson refrigeration cycles for cooling fixed-temperature heat loads. *Cryogenics*, **44**(12):847-857. [doi:10.1016/j.cryogenics.2004.05.004]

Gong, M.Q., Luo, E.C., Wu, J.F., Zhou, Y., 2004b. Study of the single-stage mixed-gases refrigeration cycle for cooling temperature-distributed heat loads. *International Journal of Thermal Sciences*, **43**(1):31-41. [doi:10.1016/S1290-0729(03)00097-8]

Gosney, W.B., 1982. Principles of Refrigeration. Cambridge University Press, London, UK,

IPPC, 2000. Third Assessment Report, Climate Change 2001. Available from http://www.grida.no/publications/other/ipcc_tar/?src=/climate/ipcc_tar/vol4/chinese/090.htm [Accessed on Dec. 25, 2008].

Khatri, A., Boiarski, M., 2008. Development of JT Coolers Operating at Cryogenic Temperatures with Nonflammable Mixed Refrigerants. AIP Conference Proceedings, **53**:3-10. [doi:10.1063/1.2908574]

Longsworth, R.C., 1994. Cryogenic Refrigerator with Single Stage Compressor. US Patent 5,337,572.

Longsworth, R.C., 1997. 80 K throttle-cycle refrigerator cost reduction. *Cryocoolers*, **9**:521-528.

Luo, E.C., Zhou, Y., Gong, M.Q., 1998. Thermodynamic analysis and optimization of 80 K closed-cycle Joule-Thomson cryocooler with gas mixture. *Advances in Cryogenic Engineering*, **43**:1679-1683.

Luo, E.C., Gong, M.Q., Wu, J.F., Zhou, Y., 2004. Properties of gas mixtures and their use in mixed-refrigerant Joule-Thomson refrigerators. *Advances in Cryogenic Engineering*, **49**:1677-1686.

Missimer, D.J., 1997. Refrigerant conversion of auto-refrigerating cascade (ARC) systems. *International Journal of Refrigeration*, **20**(3):201-207.

NIST (National Institute of Science and Technology), 2007. Standard Reference Database 23, Version 8.0.

Podbielniak, W.J., 1936. Art of Refrigeration. US Patent 2,041,725.

Ravindranatha, R.V., Senthil, K.P., Srinivasa, M.S., Venkatarathnam, G., 2006. Performance of J-T Refrigerators with Nitrogen-Argon-Helium-Hydrocarbon and Neon-Nitrogen-Hydrocarbon Mixtures. ICEC, 21, CR06-249, p.1-4.

Reynolds, W.C., 1977. Engineering Thermodynamics. McGraw-Hill, Inc., USA, p.328-329.

Rozhentsev, A., 2008. Refrigerating machine operating characteristics under various mixed refrigerant mass charges. *International Journal of Refrigeration*, **31**:1145-1155. [doi:10.1016/j.cryogenics.2004.05.004]

Rozhentsev, A., Naer, V., 2009. Investigation of the starting modes of the low-temperature refrigerating machines working on the mixtures of refrigerants. *International Journal of Refrigeration*, **32**(5):901-910. [doi:10.1016/j.ijrefrig.2008.11.005]

Walimbe, N.S., Narayankhedkar, K.G., Atrey, M.D., 2008. Experimental investigation on mixed refrigerant Joule-Thomson (MR J-T) cryocooler. *Advances in Cryogenic Engineering*, **53**:11-17.

Wang, Q., Chen, G.M., 2003. Analysis of Features of J-T Refrigeration Cycles Using Mixed Refrigerants with an Infinite Low Temperature Heat Reservoir. Cryogenics and Refrigeration-Proceedings of ICCR, Hangzhou, China, p.327-330.